A Combined Local and Nonlocal Closure Model for the Atmospheric Boundary Layer. Part II: Application and Evaluation in a Mesoscale Meteorological Model

JONATHAN E. PLEIM

Atmospheric Sciences Modeling Division, Air Resources Laboratory, National Oceanic and Atmospheric Administration, Research Triangle Park, North Carolina*

(Manuscript received 21 February 2006, in final form 11 September 2006)

ABSTRACT

A new combined local and nonlocal closure atmospheric boundary layer model called the Asymmetric Convective Model, version 2, (ACM2) was described and tested in one-dimensional form and was compared with large-eddy simulations and field data in Part I. Herein, the incorporation of the ACM2 into the fifth-generation Pennsylvania State University–NCAR Mesoscale Model (MM5) is described. Model simulations using the MM5 with the ACM2 are made for the summer of 2004 and evaluated through comparison with surface meteorological measurements, rawinsonde profile measurements, and observed planetary boundary layer (PBL) heights derived from radar wind profilers. Overall model performance is as good as or better than similar MM5 evaluation studies. The MM5 simulations with the ACM2 compare particularly well to PBL heights derived from radar wind profilers during the afternoon hours. The ACM2 is designed to simulate the vertical mixing of any modeled quantity realistically for both meteorological models and air quality models. The next step, to be described in a subsequent article, is to incorporate the ACM2 into the Community Multiscale Air Quality (CMAQ) model for testing and evaluation.

1. Introduction

The planetary boundary layer (PBL) parameterization scheme is one of the most important model components in meteorological and air quality models. Although there have been a variety of PBL schemes developed and used in mesoscale and global models, errors and uncertainties associated with these schemes remain some of the greatest sources of inaccuracies in model simulations. While PBL models are important components of meteorological models, they are even more critical components of air quality models because ground-level concentrations of pollutants are largely determined by the extent of vertical mixing. Thus, accurate and consistent simulation of the diurnal evolution and vertical mixing of meteorological and chemical species is essential for realistic simulation of these atmospheric systems.

Several studies have compared and evaluated model simulations using various PBL models. For example, Zhang and Zheng (2004) tested five different PBL schemes in the fifth-generation Pennsylvania State University–National Center for Atmospheric Research (NCAR) Mesoscale Model (MM5) simulations, including the simple nonlocal closure scheme of Blackadar (1978), an eddy diffusion scheme with a counter-gradient adjustment term known as the Medium Range Forecast (MRF) scheme (Hong and Pan 1996), and three turbulent kinetic energy (TKE) closure models: Gayno–Seaman (GS; Shafran et al. 2000), Mellor–Yamada–Janjić (MYJ; Janjić 1994), and Burke–Thompson (BT; Burke and Thompson 1989). They found a high degree of sensitivity in modeled near-surface temperature and wind speed to the choice of PBL scheme. While some of the schemes compared well to observations of temperature, all of the simulations had significant errors in wind speed. It was concluded that the Blackadar scheme performed best in these tests. A similar study by Berg and Zhong (2005) compared MM5 simulations using three of the same PBL schemes (Blackadar, MRF, GS). This study also

* In partnership with the U.S. Environmental Protection Agency.

Corresponding author address: Jonathan Pleim, Atmospheric Sciences Modeling Division, Air Resources Laboratory, NOAA, Research Triangle Park, NC 27711-0000.
E-mail: pleim.jon@epa.gov

DOI: 10.1175/JAM2534.1

showed relatively good performance by the Blackadar scheme, which compared better to observed PBL heights than did the other schemes. Another MM5 study by Vila-Guerau de Arellano et al. (2001) again found the model simulations to be very sensitive to the PBL parameterization. They also found the Blackadar scheme to perform relatively well compared to the other schemes tested (MRF, MYJ, BT). Bright and Mullen (2002) also found that better PBL structure and height were simulated by MM5 using the Blackadar or MRF schemes as compared with the TKE schemes (MYJ, BT).

All of these studies comparing various PBL parameterizations in MM5 simulations show that the simple nonlocal closure model of Blackadar generally compared better to observations than the other schemes, with the MRF, which includes a counter-gradient term, a close second. Thus, it seems that the nonlocal aspect of these schemes, which simulates counter-gradient transport by large-scale convective plumes, is more important for realistic representation of the convective boundary layer (CBL) than the higher-order closure of the TKE schemes. Conversely, Pino et al. (2003) demonstrated the important role of wind shear in the growth and maintenance of the convective boundary layer. Thus, because the Asymmetric Convective Model, version 2, (ACM2) has both local and nonlocal components, the ACM2 should produce more realistic simulations of the CBL than either the TKE schemes or pure nonlocal schemes like Asymmetric Convective Model, version 1, (ACM1) or Blackadar. Note that some nonlocal schemes, however, such as MRF, tend to overmix, which can result in the CBL being too deep, warm, and dry. For example, Braun and Tao (2000) found that excessive mixing by MRF weakened the simulated development of Hurricane Bob. Wisse and de Arellano (2004) also showed the strong interaction of the PBL scheme with severe precipitation events where the MRF scheme enhanced precipitation area and amount by stronger and deeper vertical mixing than the Eta or Blackadar schemes. Thus, it seems that while nonlocal components are important for simulating the effects of large-scale convective eddies, realistic apportionment of fluxes between local and nonlocal components is critical for realistic CBL mixing and depth.

Pleim (2007, hereinafter Part I) demonstrated the capabilities of the ACM2 in one-dimensional tests where the initial conditions and surface and geostrophic forcing could be precisely prescribed. While those tests showed very accurate responses, it is still essential to validate overall performance of three-dimensional modeling systems with the ACM2 used for the PBL parameterization. Section 2 describes the implementation of the ACM2 in the MM5, including the detailed formulation of the eddy diffusivities used and the numerical integration techniques. The specifics of the MM5 simulations used for testing and evaluation are summarized in section 3. This section also presents the evaluation of the MM5 applications of the ACM2 through comparison of model results with surface, profile, and PBL height observations. Last, a few conclusions are offered in section 4.

2. Application of ACM2 in MM5

The mathematical formulation of the ACM2 scheme, along with demonstrations of its performance in one-dimensional tests, is presented in Part I. Additional description and a formulation relevant to the incorporation of the ACM2 into MM5 is provided here, including the complete eddy diffusivity formulation and numerical integration techniques.

The Pleim–Xiu land surface model (PX LSM) (Pleim and Xiu 1995; Xiu and Pleim 2001; Pleim and Xiu 2003) has been an option in MM5 since version 3.4, which was first released in 2001. The original ACM (Pleim and Chang 1992) is included in this option and, until recently, was the only PBL option that could be used with the PX LSM. For the experiments discussed here, the new ACM2 replaces the ACM within the PX LSM option. In addition to the enhanced mixing scheme, which now includes both local and transilient mass fluxes, other differences between the ACM MM5 application and the ACM2 MM5 application include a modified scheme for diagnosis of PBL height (described in Part I), a more complex but computationally efficient matrix solver for semi-implicit integration, and an upgraded eddy diffusivity scheme that combines boundary layer scaling and local shear and stability-based formulations.

a. Eddy diffusivity

The ACM2 requires eddy diffusivities for all stability conditions both within and above the PBL. Above the PBL eddy diffusivity is based on local wind shear and stability while within the PBL a boundary layer scaling formulation for eddy diffusivity is defined similarly to Holtslag and Boville (1993) as

$$K_z(z) = k \frac{u_*}{\phi\left(\frac{z_s}{L}\right)} z(1 - z/h)^2, \tag{1}$$

where k is the von Kármán constant ($k = 0.4$), u_* is the friction velocity, and h is the PBL height. For unstable conditions, the height used in the stability function

(z_s/L) is capped at the top of the surface layer [z_s = min(z, 0.1 h)], whereas for stable conditions the actual height is always used ($z_s = z$). The nondimensional profile functions of heat (ϕ_h) and momentum (ϕ_m) for unstable conditions, according to Dyer (1974), are given by

$$\phi_h = \left(1 - 16\frac{z}{L}\right)^{-1/2} \quad \text{and}$$

$$\phi_m = \left(1 - 16\frac{z}{L}\right)^{-1/4}, \tag{2}$$

and for stable conditions

$$\phi_h = \phi_m = 1 + 5\frac{z}{L},$$

where the Monin–Obukov length scale L is

$$L = \frac{T_o u_*^2}{gk\theta_*}. \tag{3}$$

Here T_o represents the average temperature in the surface layer, and θ_* is the surface temperature scale defined as the surface kinematic heat flux divided by u_*.

The boundary layer scaling form of K_z [Eq. (1)] only applies within the PBL; therefore, it is necessary to have alternate formulations for eddy diffusivity independent from PBL and surface-based parameters. Following the example of Liu and Carroll (1996) and others, expressions for eddy diffusivity as functions of wind shear and local Richardson number are derived as

$$K_z = K_{zo} + \left|\frac{\partial U}{\partial z}\right|\left(1 - \frac{\text{Ri}}{\text{Rc}}\right)^2 l_s \tag{4a}$$

for stable conditions (Ri > 0), and

$$K_z = K_{zo} + \left[\left(\frac{\partial U}{\partial z}\right)^2 (1 - 0.25\text{Ri})\right]^{0.5} l_s \tag{4b}$$

for unstable conditions, where K_{zo} is the minimum K_z, which is set to 0.05 m^2 s^{-1}, and Rc is the critical Richardson number set to 0.25. The length scale l_s is defined such that it increases with height above ground but then levels off asymptotically to a constant value ($\lambda = 80$ m),

$$l_s = \left(\frac{kz\lambda}{kz + \lambda}\right)^2. \tag{5}$$

As with the implementation of the Blackadar PBL scheme in MM5 (see Grell et al. 1994), local Richardson number is defined in either one of two ways, depending on whether or not condensed cloud water is present. When cloud water is not present the Richardson number at the interface between layer i and $i + 1$ is

$$\text{Ri}_{i+(1/2)} = \frac{g}{\theta_{i+(1/2)}}\left(\frac{\Delta\theta}{\Delta z}\right)_{i+(1/2)}\left(\frac{\Delta U}{\Delta z}\right)^{-2}_{i+(1/2)}. \tag{6a}$$

If either cloud water mixing ratio q_c or cloud ice mixing ratio q_i are greater than zero, Ri is defined according to Durran and Klemp (1982) as

$$\text{Ri}_{i+(1/2)} = (1 + \alpha)\left[\text{Ri}_{\text{dry}} - \frac{g^2}{C_p T_{i+(1/2)}}\left(\frac{\Delta U}{\Delta z}\right)^{-2}_{i+(1/2)}\frac{(\chi - \alpha)}{(1 + \chi)}\right], \tag{6b}$$

where Ri_{dry} is the dry Richardson number as computed by (6a),

$$\chi = \frac{L_v^2 q_{v[i+(1/2)]}}{C_p R_v T^2_{i+(1/2)}} \quad \text{and} \tag{6c}$$

$$\alpha = \frac{L_v^2 q_{v[i+(1/2)]}}{R_d T_{i+(1/2)}}. \tag{6d}$$

Variables such as T, θ, and q_v, with the subscript $i + (1/2)$, represent averages of the variable in layer i and $i + 1$. In addition, L_v is the latent heat of vaporization and R_d and R_v are the ideal gas constants for dry air and water vapor, respectively.

In general, within the PBL, the boundary layer scaling K_z [Eq. (1)] is greater than the local formulation [Eq. (4)]. However, near the top of the PBL, as z approaches h, the K_z computed according to the boundary layer scaling scheme approaches zero. While the top of the PBL is usually in a stable inversion layer, it is also often characterized by high wind shear. Therefore, it makes sense to allow the K_z to be determined by the local scheme, which is sensitive to wind shear, even within the PBL. Thus, the maximum of the two methods of K_z calculation is applied during unstable conditions within the PBL. The one-dimensional testing, comparing the ACM2 with LES experiments, described in Part I, showed better agreement at the top of the PBL when the maximum K_z was applied. The one-dimensional experiments comparing the ACM2 with CASES-99 observations also showed good agreement near the top of the PBL.

Because the Cooperative Atmosphere and Surface Exchange Study in 1999 (CASES-99) experiments were multiday simulations, stable nocturnal performance was also assessed. For this experiment the best results were obtained when the boundary layer scaling scheme only was used for the stable boundary layer (SBL). Therefore, even though one might expect the local scheme to be more sensitive to wind shear, which is typically the primarily source of turbulence in stable conditions, the boundary layer scaling approach was used within the SBL for the MM5 simulations.

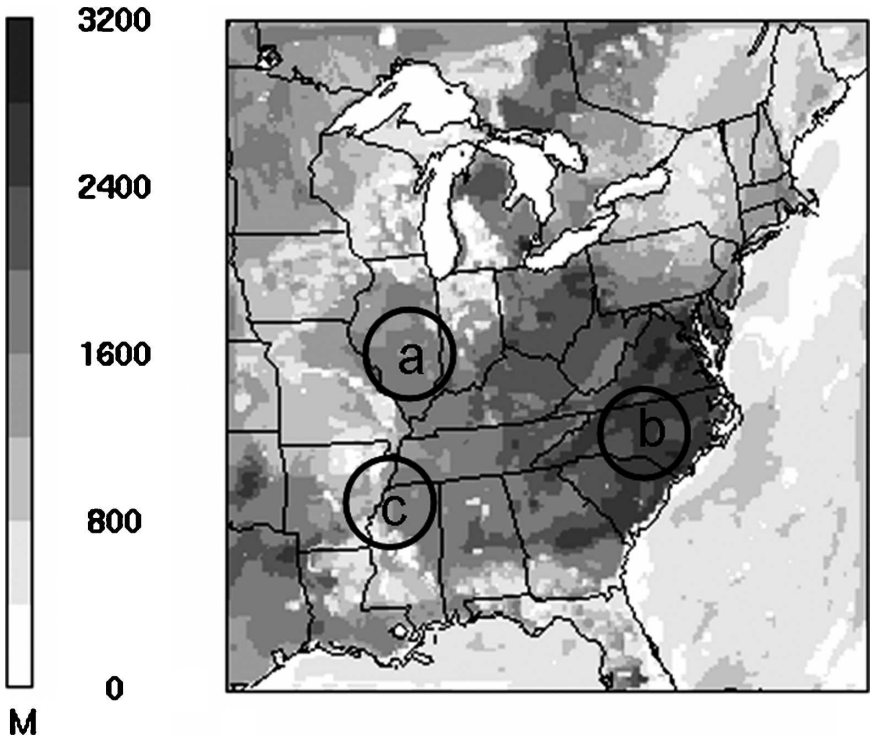

FIG. 1. Example of PBL height simulated by MM5–ACM2 for the full 12-km modeling domain at 1900 UTC 16 Jul 2004. The circles designated "a," "b," and "c" represent 200-km radius areas over which the time series shown in Fig. 2 are averaged.

b. Numerical integration

For application in three-dimensional numerical grid models it is important to balance complexity with efficiency. Thus, a computationally efficient, stable, and accurate numerical integration solver is essential for operational use in meteorological and air quality models. Typically, semi-implicit integration techniques are used to solve first-order PBL model equations. Semi-implicit integration techniques, such as Crank–Nicholson, where the past and future time steps are equally weighted, are absolutely stable and very accurate. For eddy diffusion schemes (even with the nonlocal gradient adjustment term), simple and efficient tridiagonal matrix solvers are usually used. Simple nonlocal closure models such as the Blackadar convective scheme (Blackadar 1978) or the original ACM can be integrated using semi-implicit techniques by solution of very sparse matrices that are as simple and efficiently solved as a tridiagonal matrix. On the other hand, full transilient matrix models, such as that described by Stull (1984), would require more computationally intensive matrix inversion techniques, such as lower–upper (LU) decomposition for semi-implicit integration. The ACM2 presents an intermediate challenge for numerical integration.

The matrix solver developed for the ACM2 is a simplified LU decomposition. The matrix that results from the semi-implicit form of the finite difference equations is a border-band tridiagonal matrix or tridiagonal plus the first column. Application of the LU decomposition technique results in a filled lower matrix, but only a bidiagonal upper matrix. Thus, the semi-implicit integration of the ACM2 model is more computationally expensive than the original ACM or eddy diffusion models but cheaper than a full transilient matrix model. Furthermore, by optimizing the loop structure of the code the MM5 application of the ACM2 adds very little to the overall model's execution time.

3. Testing ACM2 in MM5

The ACM2 was incorporated into MM5, version 3.7.2, by replacing the ACM in the PX LSM option. Otherwise, the model configuration was similar to that used for several other modeling studies where MM5 was run retrospectively to provide meteorological fields for subsequent air quality modeling (e.g., Gilliam et al. 2006). In addition to the PX LSM, the other physics options included the rapid radiation transfer model (RRTM) for longwave radiation (Mlawer et al. 1997),

TABLE 1. Model performance statistics for the 12-km MM5–ACM2 simulations over the period of 13 Jul–18 Aug 2004.

	T	q_v	Wind speed	Wind direction
Data count	398 848	398 848	398 848	398 848
Correlation	0.934	0.915	0.612	—
MAE	1.42 K	1.14 g kg^{-1}	1.026 m s^{-1}	31.8°
MB	0.369 K	0.109 g kg^{-1}	−0.211 m s^{-1}	10.2°
IA	0.931	0.911	0.606	—

version 2 of the Kain–Fritsch (KF2) cumulus parameterization (Kain 2004), and the Reisner 2 microphysics scheme (Reisner et al. 1998). Four-dimensional data assimilation (FDDA) was applied using gridded analyses for nudging winds at all levels and temperature and humidity above the PBL. Also, the indirect nudging of soil moisture using surface analyses of temperature and humidity was used with the PX LSM as described by Pleim and Xiu (2003).

MM5 simulations were run for the period of July 13 through 18 August 2004 at 12-km grid resolution on a domain that extended from Maine in the northeast to eastern Texas in the southwest. Figure 1 shows the computational domain and an example of modeled PBL height at 1900 UTC 16 July 2004. Initial and lateral boundary conditions were derived from Eta analyses at 6-h intervals with 3-h Eta forecasts in between that were provided by the National Centers for Environmental Prediction (NCEP). The Eta analyses and forecasts were also processed through the "little r" preprocessor for reanalysis adding all available surface observations for use in FDDA.

The purpose of this analysis is to evaluate the ACM2 when it is used in MM5. Many components other than the PBL model, however, affect the accuracy of MM5 simulations. Thus, it is difficult to assess the capabilities of any single model component, such as a new PBL model, through evaluation of MM5 results. The performance of the ACM2 has already been demonstrated in a stand-alone form through comparisons with LES and field experiment data as reported in Part I. The goal here is to see if MM5 simulations that include the ACM2 PBL scheme show acceptable performance when evaluated against observations, that is, similar to other MM5 evaluation studies. Thus, the model evaluation focuses on parameters most directly affected by the PBL parameterization. Comparisons are made with profiles of potential temperature and humidity measured by rawinsondes and PBL heights derived from radar profiles. Comparisons with surface data are also valuable because of the great number of stations and hourly data archives.

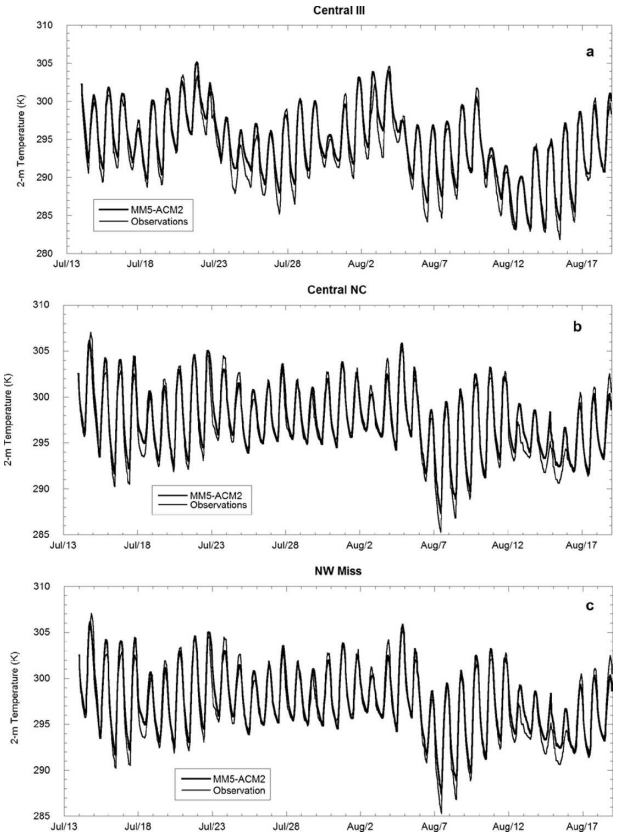

FIG. 2. Modeled and measured 2-m temperature averaged over all NWS–FAA sites within 200-km radius circles centered in (a) central Illinois, (b) central North Carolina, and (c) northwest Mississippi as shown in Fig. 1.

Note that this study does not attempt to show superiority over the other PBL models available in the MM5 system because the different PBL schemes are integrated with different LSMs, making clean PBL comparisons impossible without major recoding. Surface fluxes of heat and humidity, in particular, are primarily products of the LSM. Thus, surface level temperature and humidity, as well as PBL heights, are influenced as much by the LSMs as by the PBL models. Clean comparisons, in which the same LSM and surface flux-profile schemes are used with different PBL models, will be possible once the ACM2 has been included in the WRF system where the PBL, surface scheme, and LSM are in different modules and thus are more easily interchangeable.

a. Surface evaluation

The MM5 simulations were compared with the surface measurements from all available National Weather Service (NWS) and Federal Aviation Administration (FAA) sites. Table 1 summarizes the statistical com-

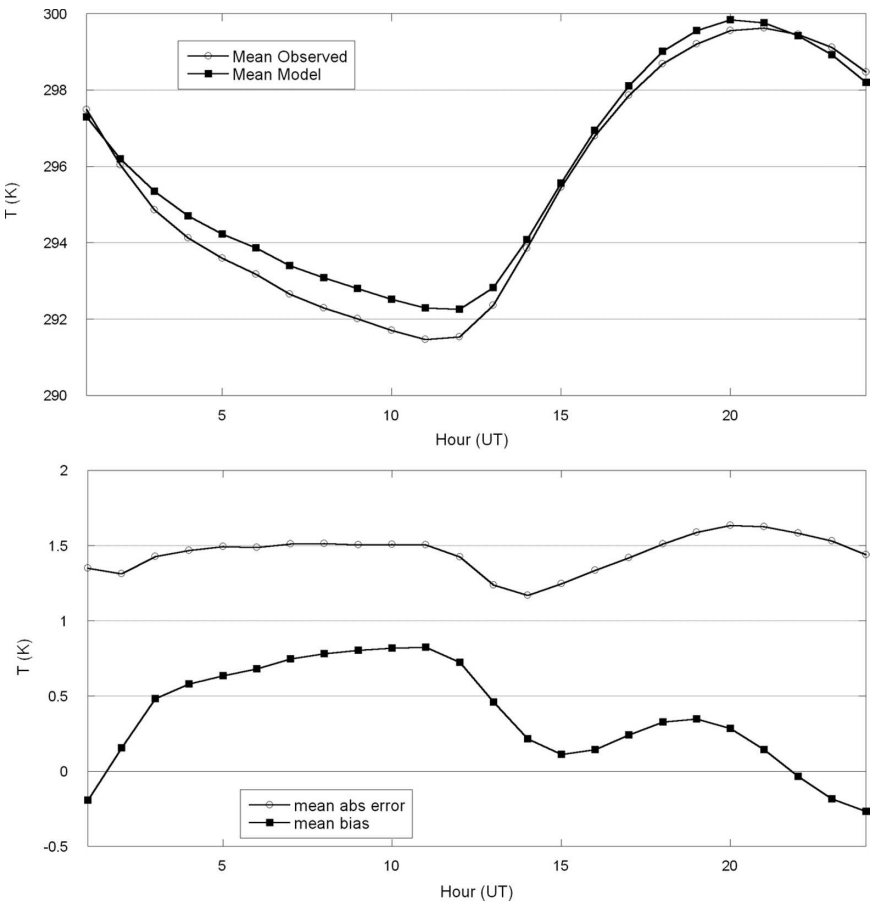

FIG. 3. (top) Modeled and measured 2-m temperature averaged over all sites and the entire modeling period and (bottom) mean bias and mean absolute error between modeled and measured 2-m temperature averaged over all sites and the entire modeling period.

parisons for temperature and humidity mixing ratio at 2 m and wind speed and direction at 10 m. The statistics shown are data count, correlation, mean absolute error (MAE), mean bias (MB), and index of agreement (IA), which is a measure of how well the model represents patterns of variation about the mean (Wilks 1995). To give some context it is helpful to compare these statistics with other similar model evaluation studies. The most comparable modeling study was a two-domain nested simulation at 36 and 12 km for 2001 that was analyzed and reported by Gilliam et al. (2006). The MM5 physics configuration for that study was very similar to the current study, including the RRTM, Reisner 2, KF2, and PX LSM using the original ACM. Statistics for the MM5–ACM2 simulation compared favorably with the summer 12-km results reported by Gilliam et al. (2006). For 2-m temperature, the MM5–ACM2 simulation showed better MAE (1.42 vs 1.99), slightly better MB (0.37 vs 0.41), and nearly the same IA (0.93 vs 0.92). The 10-m wind speed statistics also compared well to the results of the Gilliam study with greater but still small MB (−0.21 vs −0.10), and slightly better MAE (1.03 vs 1.15) and IA (0.61 vs 0.49). Humidity and wind direction statistics were not reported by Gilliam et al. (2006). The humidity statistics show very good agreement with surface measurements with very small bias (0.11 g kg^{-1}) and favorable MAE (1.14 g kg^{-1}) and IA (0.91). Wind direction statistics, however, show fairly large values of MAE (31.8°) and MB (10.2°). Note that such errors are common for wind direction in midsummer conditions when winds are often light and variable. Overall, these statistics are similar to the results of other recent MM5 evaluation studies that used the original ACM (Abraczinskas et al. 2004; Baker et al. 2005), and another that used the MRF PBL model (Mass et al. 2003)

Additional insight into model performance can be revealed by a comparison of spatially averaged time series and domain-averaged diurnal time series. Figure 2 shows three time series of measured and modeled 2-m

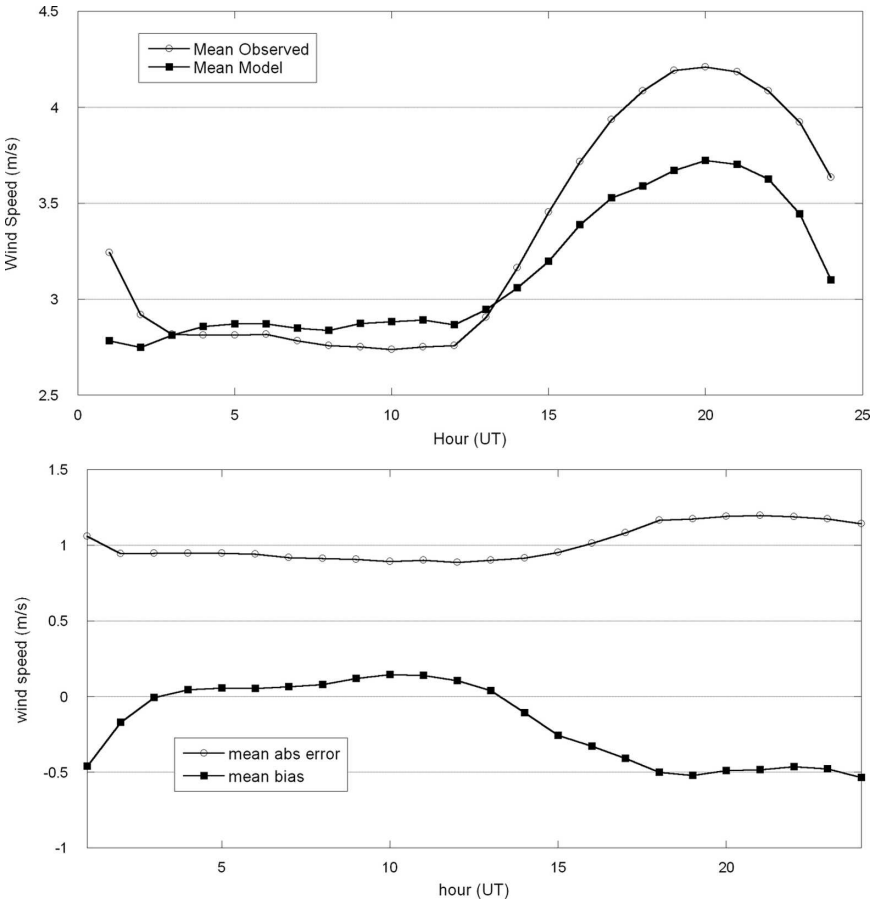

FIG. 4. (top) Modeled and measured 10-m wind speed averaged over all sites and the entire modeling period and (bottom) mean bias and mean absolute error between modeled and measured 10-m wind speed averaged over all sites and the entire modeling period.

temperature averaged over all NWS–FAA sites within circular areas of 200-km radius. The area represented in the top panel is centered in the middle of Illinois, the middle panel is centered in central North Carolina, and the bottom in northwestern Mississippi. Daytime maximum temperatures were often accurately modeled. For more than one-half of the days the maximum model temperature was within 1 K of the observed. On days with larger errors in maximum temperature, warm and cold biases are about evenly split. Such errors are often attributable to errors in cloud cover or soil moisture. All three time series show a frequent nighttime warm bias, especially during the cooler and more stable nights. Possible reasons for this warm bias include a minimum eddy diffusivity that is too large, leading to excessive downward mixing into the ground-based inversion, and deep soil temperatures that are too warm, thus restraining surface radiational cooling. Note that warm biases in daily minimum temperature are a common feature of mesoscale models in the summer (e.g., Zhong et al. 2005). Steeneveld et al. (2006) found that MM5 overpredicted temperature using either the MRF or Eta PBL schemes during very stable nights with intermittent or nearly absent turbulence, but compared well on a fully turbulent night. They demonstrated, using a single-column model with high vertical resolution in both the soil and atmosphere, that all three nights could be accurately simulated when coupled to a vegetation layer. Research into improved stable boundary layer modeling will be the subject of future work.

The upper panel of Fig. 3 shows diurnal time series of 2-m temperature averaged over all days and all sites in the modeling domain. It is clear from these results that the model has a significant warm bias at night but very little bias in the daytime temperatures. Note that the daytime results are the more important validation of the ACM2 because the combined local and nonlocal transport scheme is only activated for unstable conditions. The statistics shown in the lower panel of Fig. 3 demonstrate that the mean biases from the late morn-

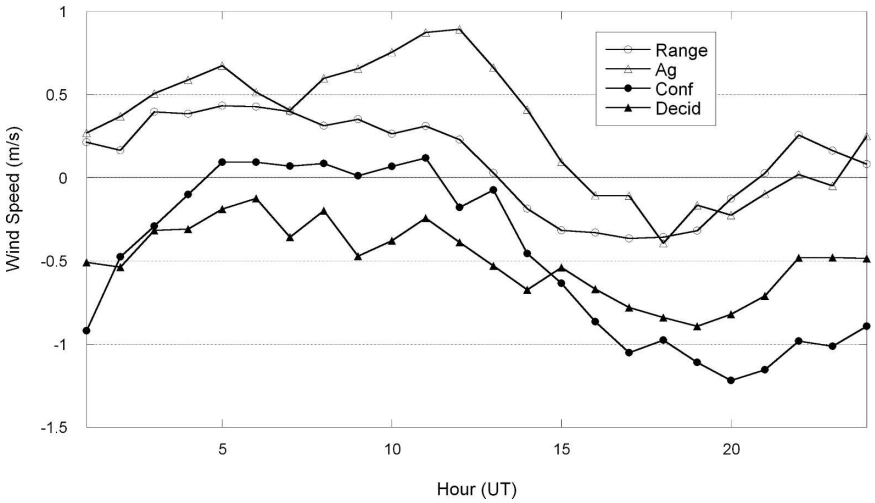

FIG. 5. Mean bias of modeled 10-m wind speed at selected sites where dominant model land use is rangeland, agricultural, coniferous, and deciduous.

ing through the evening hours are within approximately $\pm 1/3$ K. Also, the mean absolute error is less than 1.7 K for every hour.

Comparisons of mean 10-m wind speed are presented in Fig. 4. The upper panel of Fig. 4 shows strong diurnal signals for both the observed and modeled wind speed. The amplitude of this signal, however, is underrepresented by the model, resulting in a slight positive bias at night and a more substantial negative bias in the daytime. Note that Zhang and Zheng (2004) found a similar tendency toward positive wind speed bias at night and negative bias in the daytime in tests of five different PBL schemes used in MM5 simulations. Even with this underpredicted diurnal amplitude, the statistics presented in the lower panel of Fig. 4 show that the mean bias is within approximately $\pm 0.5 \text{m s}^{-1}$, with mean absolute error $<1.2 \text{ m s}^{-1}$ for all hours.

The slight positive wind bias at night is consistent with the warm bias at night and suggests deficiencies in the stable PBL parameterizations as noted above. The daytime negative wind speed bias could possibly be explained by the predominance of airport measurement sites, which tend to be in large open areas. Thus, the roughness lengths of model grid cells collocated with the observation sites are generally greater than for the airport measurement sites, resulting in greater surface drag in the model that would tend to slow the 10-m winds. If this hypothesis is correct we would expect

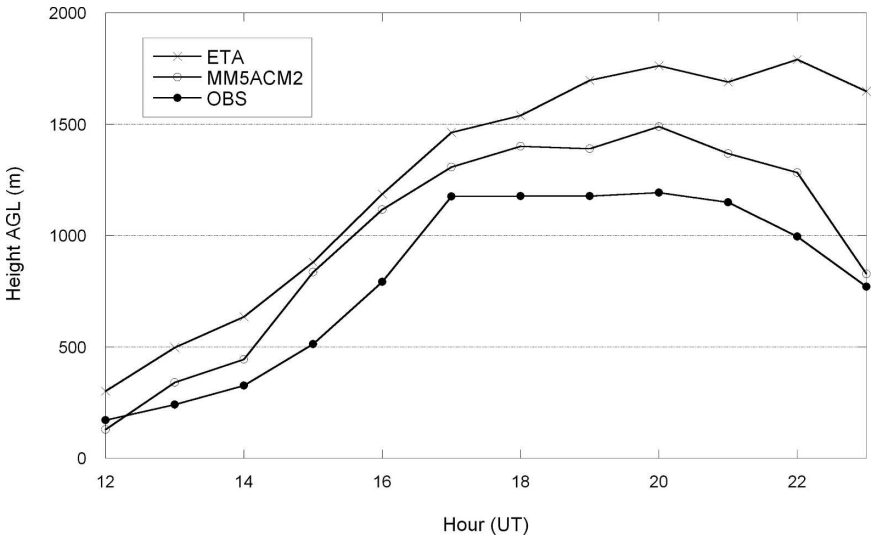

FIG. 6. PBL height averaged over the simulation period from the MM5–ACM2 and Eta models and derived from a radar wind profiler at Pittsburgh.

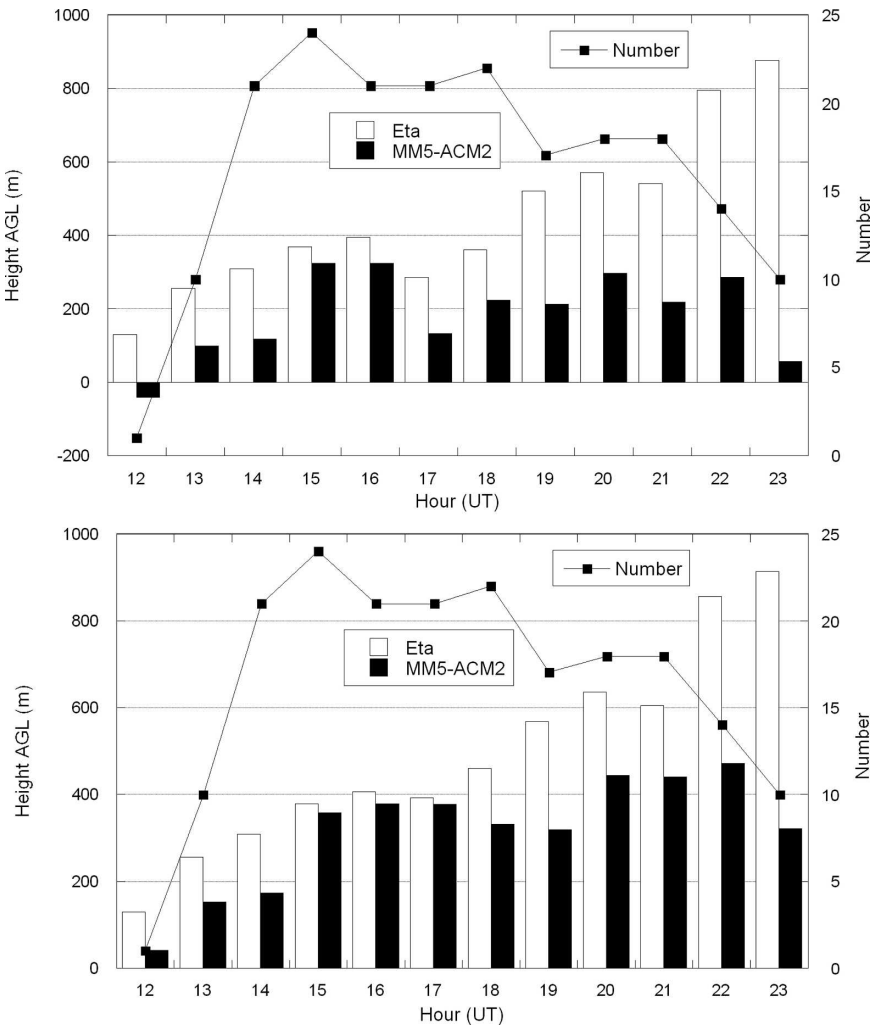

FIG. 7. (top) Mean bias and (bottom) mean absolute error for MM5–ACM2 and Eta PBL height simulations at Pittsburgh. Also, the number of observed data points available for each hour shown in both panels.

daytime negative biases to be greatest in heavily forested areas and less in open areas. Figure 5 shows wind speed biases grouped by the dominant land use in the collocated model grid cell. In forested areas, both deciduous and coniferous, the daytime negative biases are even greater than the overall statistics. In more open areas, both agricultural and rangeland, the daytime negative biases are smaller. Considering that the roughness is more similar between model grid cell and measurement site in the more open areas, these results tend to validate the convective scheme for wind speed.

b. Profiles and PBL heights

Frequent vertical profiles of potential temperature, humidity, and winds through the lowest few kilometers of the atmosphere would be the most relevant observed data for PBL evaluation. Rawinsondes measure such profiles but they are generally launched only twice daily at 0000 and 1200 UTC. Radar wind profiler data are generally available on an hourly frequency, but only provide vertical profiles of winds, which are not the best for PBL evaluation because they are usually more influenced by model dynamics than PBL mixing. While some profilers also report temperature from a coincident radio acoustic sounding system, these data do not reach high enough for useful PBL analysis. A very valuable product that can be reliably derived from radar profilers is the hourly PBL height. Unfortunately, this is not yet routinely calculated and archived. However, there has been an effort to estimate PBL height for several sites in the northeast United States for the International Consortium for Atmospheric Research on

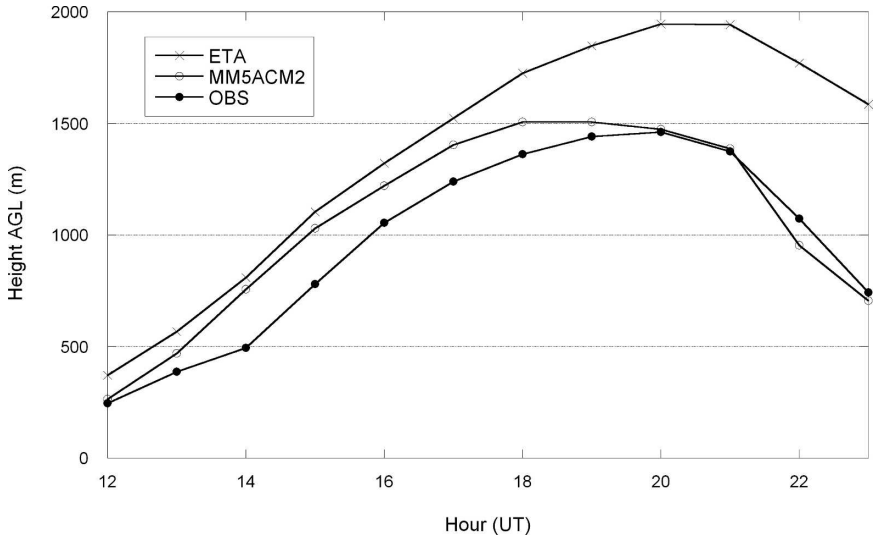

FIG. 8. PBL height averaged over the simulation period from the MM5–ACM2 and Eta models and derived from a radar wind profiler at Concord.

Transport and Transformation experiment during the summer of 2004. Comparisons with these data for two of the sites that are sufficiently inland to avoid coastal effects can demonstrate the ability of the model to simulate accurate PBL heights.

Figures 6–9 present comparisons between model simulations of PBL height and PBL heights derived from radar wind profilers at two sites—Pittsburgh, Pennsylvania, and Concord, New Hampshire. The observed PBL heights were hand analyzed using a combination of signal-to-noise ratio (Angevine et al. 1994) and vertical velocity variance (Bianco and Wilczak 2002). Observations of PBL height are included in the analysis only when the techniques are least ambiguous, which is generally for daytime cloud-free conditions. For reference, PBL heights from the NCEP Eta Model forecasts are also shown. Figures 6 and 8 show the PBL heights simulated by the two models and the profiler-derived estimates averaged over all available data for each hour of the day. The number of data points for each hour is shown in Figs. 7 and 9 along with the mean bias and mean absolute error for the two models. The number of data points for each hour, which are greatest during the midday hours when the top of the PBL is most readily defined, is generally more than half of the 35 days of the modeling period. Note that the decline in data count for the mid- to late-afternoon hours reflects the greater amount of cloud cover at these times.

At both sites the MM5–ACM2 PBL heights, like the Eta PBL heights, tend to overestimate the PBL height during the morning hours. Another way to interpret these plots is that the models tend to simulate the morning rise in PBL height too quickly. This morning high bias in PBL height is consistent with the nighttime and early morning warm biases shown in Fig. 3. During the afternoon hours, however, the gap between the MM5–ACM2 PBL heights and the observations narrows, while Eta's high bias increases. Indeed, at the Concord site, the mean bias virtually disappears in the afternoon, although MAE values persist at around 400–600 m at Concord and around 400 m at Pittsburgh.

These limited results suggest that the model is capable of realistic simulation of PBL heights. The morning high bias at both sites is more likely caused by the early morning warm bias than caused by a limitation in the ACM2 scheme. The fact that the high biases tend to decrease in the afternoon suggests that the convective simulation is not inherently overactive. Recall that the LES comparisons described in Part I showed very good agreement for PBL height with a very slight low bias. Also, the close agreement with observations during the evening PBL height decline is a sign that the model is producing realistic PBL mixing. Note that the premature collapse of the PBL has been a problem in air quality modeling resulting in erroneous spikes in evening chemical concentrations (Dennis et al. 2007). It will be interesting to see if this problem is ameliorated when the ACM2 is tested in the Community Multiscale Air Quality (CMAQ) model.

The most rigorous evaluation of a PBL model would be through a comparison with observed vertical profiles at all times of the day. Unfortunately, the rawinsonde network regularly reports only 2 times per day. Comparisons of model results with 0000 UTC soundings can

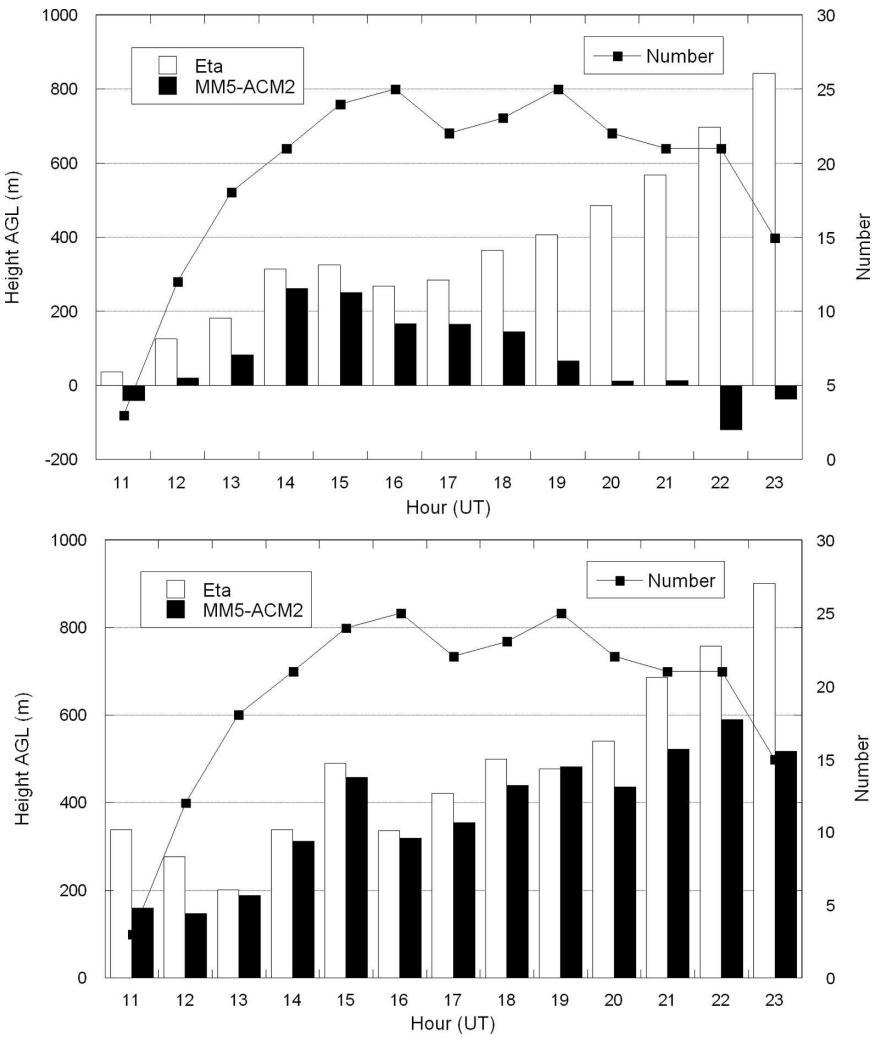

FIG. 9. (top) Mean bias and (bottom) mean absolute error for MM5–ACM2 and Eta PBL height simulations at Concord. Also, the number of observed data points available for each hour shown in both panels.

be valuable for evaluation of late-afternoon profiles, particularly in the western portion of the domain where the local time is 1900. Figures 10 and 11 show examples of vertical profiles of potential temperature and relative humidity produced by MM5–ACM2 and derived from rawinsonde measurements. Both rawinsonde sites are in the western part of the domain in the central time zone—Minneapolis, Minnesota (Fig. 10), and Little Rock, Arkansas (Fig. 11). The weather during the afternoon of 5 August, leading up to the sounding at 0000 UTC 6 August shown in Fig. 10, was completely clear in the Minneapolis area with northeast winds at about 1–2 m s^{-1}. Similarly, the weather during the afternoon of 6 August, leading up to the 0000 UTC 7 August sounding, shown in Fig. 11, was completely clear in the Little Rock vicinity with northeast wind around 4 m s^{-1}. Both profiles show very close comparisons between observed and modeled potential temperature and relative humidity. This is not to suggest that the model always compares so closely with rawinsonde profiles. However, it is under such low wind speed, clear-sky conditions that the PBL scheme would be expected to have the greatest influence on modeled vertical profiles. Thus, good performance under these conditions demonstrates realistic PBL simulation capability.

4. Conclusions

The ability to simulate the turbulent vertical transport by both small-scale shear-driven turbulence and large-scale convective turbulence seems to be essential for realistic modeling of the convective boundary layer.

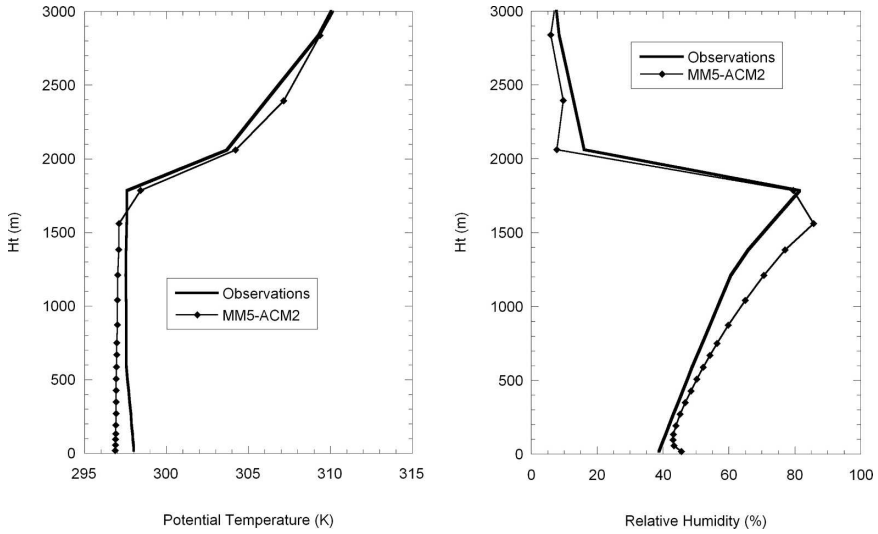

FIG. 10. Modeled profiles of (left) potential temperature and (right) relative humidity in comparison with rawinsonde measurements at Minneapolis at 0000 UTC 6 Aug 2004.

Part I of this pair of articles demonstrated that the ACM2 is able to closely reproduce vertical profiles from large-eddy simulations of idealized experiments. Evaluation of the ACM2 as a component of an MM5 simulation is more difficult, both because the data used for comparison are much less comprehensive, and because errors in other components of the model also affect the results. Thus, much of the analysis presented here focuses on averaged and statistical comparisons, with the intention of identifying persistent biases and errors that may be attributable to the PBL scheme.

The 2-m temperature comparisons show a significant warm bias in nocturnal temperatures, but very little bias in daytime temperatures. The cause of the nighttime warm bias may be related to the stable eddy diffusion scheme, but it may also be related to the land

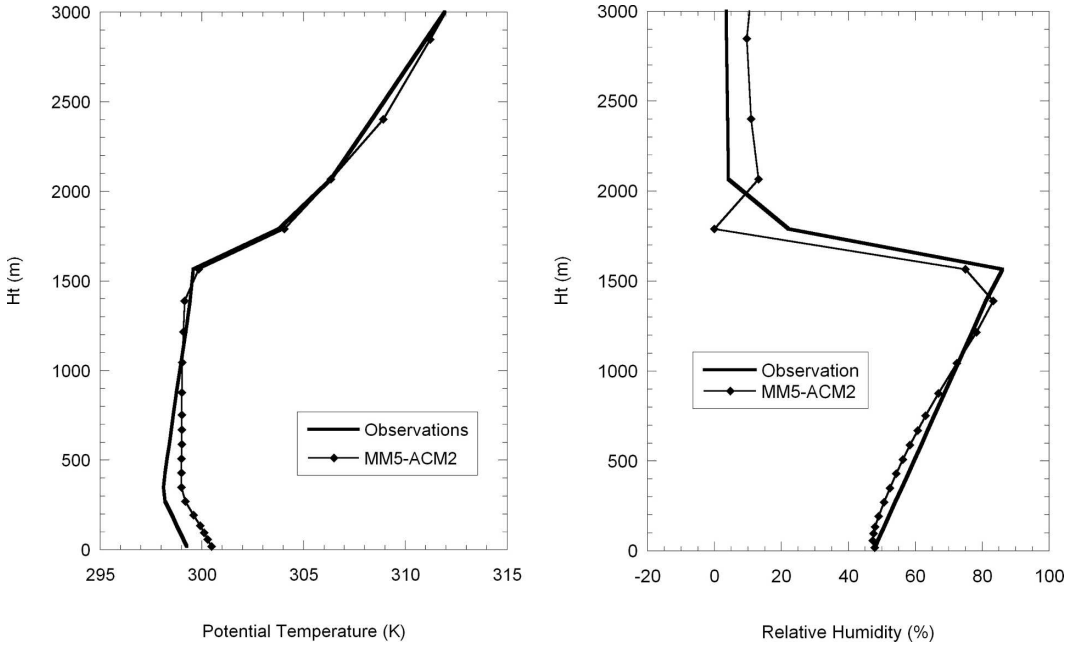

FIG. 11. Modeled profiles of (left) potential temperature and (right) relative humidity in comparison with rawinsonde measurements at Little Rock at 0000 UTC 7 Aug 2004.

surface model, particularly the soil temperature. The afternoon results, however, are very encouraging with respect to the convective scheme. The wind speed statistics also support the validity of the ACM2 for convective boundary layer mixing, particularly when stratified by dominant land use to account for the roughness disparity between measurement sites and model grid cells.

Surface statistics are only part of the validation of a PBL model. The daily growth, maximum height, and evening collapse of the PBL are critical for both meteorological and air quality modeling. The comparisons with limited PBL height observations lend credence to the accuracy of the ACM2. The close comparisons with rawinsonde profiles during clear, low-wind conditions also tend to validate the PBL algorithm for convective conditions.

The next step is the evaluation of the ACM2 in an air quality model, namely, the CMAQ model. The particular advantage of the ACM2 over eddy diffusion schemes with a counter-gradient adjustment term (e.g., Holtslag and Boville 1993; Troen and Mahrt 1986; Noh et al. 2003) is its applicability to any quantity, either meteorological or chemical. While the latter type of model has been very successful for meteorological modeling, it is not clear how it can be extended to atmospheric chemistry modeling because the counter-gradient term is directly related to the surface flux of the modeled variable. This makes sense for heat or moisture, which involve turbulent surface fluxes, but not for chemical species where surface sources are often pollutant emissions that are not related to turbulent fluxes. The ACM2, on the other hand, is a mass flux scheme that does not depend on the surface sources or sinks and can easily accommodate any source/sink profile, including elevated sources.

Acknowledgments. The author thanks Jim Wilczak and Laura Bianco for deriving and providing the PBL heights from radar wind profiler measurements. The author also gratefully acknowledges the assistance of Robert Gilliam in the statistical comparisons between model results and meteorological observations. The research presented here was performed under the Memorandum of Understanding between the U.S. Environmental Protection Agency (EPA) and the U.S. Department of Commerce's National Oceanic and Atmospheric Administration (NOAA) and under Agreement DW13921548. This work constitutes a contribution to the NOAA Air Quality Program. Although it has been reviewed by EPA and NOAA and approved for publication, it does not necessarily reflect their policies or views.

REFERENCES

Abraczinskas, M. A., D. T. Olerud, and A. P. Sims, 2004: Characterizing annual meteorological modeling performance for visibility improvement strategy modeling in the southeastern U.S. Preprints, *13th Conf. on the Applications of Air Pollution Meteorology with the Air and Waste Management Association,* Vancouver, BC, Canada, Amer. Meteor. Soc., CD-ROM, 5.1.

Angevine, W. M., A. B. White, and S. K. Avery, 1994: Boundary layer depth and entrainment zone characterization with a boundary layer profiler. *Bound.-Layer Meteor.,* **68,** 375–385.

Baker, K., M. Johnson, S. King, and W. Ji, 2005: Meteorological modeling performance summary for application to PM2.5/haze/ozone modeling projects. Lake Michigan Air Directors Consortium, Midwest Regional Planning Organization, Des Plaines, IL, 72 pp. [Available online at http://www.ladco.org/tech/photo/docs/MM5_MPE_feb2005_binder.pdf.]

Berg, L. K., and S. Zhong, 2005: Sensitivity of MM5-simulated boundary layer characteristics to turbulence parameterizations. *J. Appl. Meteor.,* **44,** 1467–1483.

Bianco, L., and J. M. Wilczak, 2002: Convective boundary layer depth: Improved measurement by Doppler radar wind profiler using fuzzy logic methods. *J. Atmos. Oceanic Technol.,* **19,** 1745–1758.

Blackadar, A. K., 1978: Modeling pollutant transfer during daytime convection. Preprints, *Fourth Symp. on Atmospheric Turbulence, Diffusion, and Air Quality,* Reno, NV, Amer. Meteor. Soc., 443–447.

Braun, S. A., and W.-K. Tao, 2000: Sensitivity of high-resolution simulations of Hurricane Bob (1991) to planetary boundary layer parameterizations. *Mon. Wea. Rev.,* **128,** 3941–3961.

Bright, D. R., and S. L. Mullen, 2002: The sensitivity of the numerical simulation of the southwest monsoon boundary layer to the choice of PBL turbulence parameterization in MM5. *Wea. Forecasting,* **17,** 99–114.

Burke, S. D., and W. T. Thompson, 1989: A vertically nested regional numerical weather prediction model with second-order closure physics. *Mon. Wea. Rev.,* **117,** 2305–2324.

Dennis, R., S. Roselle, R. Gilliam, and J. Arnold, 2007: High time-resolved comparisons for in-depth probing of CMAQ fine particle and gas predictions. *Air Pollution Modeling and Its Applications, XVII,* C. Borrego and A.-L. Norman, Eds., Springer, 515–524.

Durran, D. R., and J. B. Klemp, 1982: The effects of moisture on trapped mountain lee waves. *J. Atmos. Sci.,* **39,** 2152–2158.

Dyer, A. J., 1974: A review of flux-profile relationships. *Bound.-Layer Meteor.,* **7,** 363–372.

Gilliam, R. C., C. Hogrefe, and S. T. Rao, 2006: New methods for evaluating meteorological models used in air quality applications. *Atmos. Environ.,* **40,** 5073–5086.

Grell, G. A., J. Dudhia, and D. Stauffer, 1994: A description of the fifth-generation Penn State/NCAR Mesoscale Model (MM5). NCAR Tech. Note TN-398 + STR, 138 pp.

Holtslag, A. A. M., and B. A. Boville, 1993: Local versus nonlocal boundary layer diffusion in a global climate model. *J. Climate,* **6,** 1825–1842.

Hong, S. Y., and H. L. Pan, 1996: Nonlocal boundary layer vertical diffusion in a Medium-Range Forecast model. *Mon. Wea. Rev.,* **124,** 2322–2339.

Janjić, Z. I., 1994: The step-mountain Eta coordinate model: Further developments of the convection, viscous sublayer, and turbulence closure schemes. *Mon. Wea. Rev.,* **122,** 928–945.

Kain, J. S., 2004: The Kain–Fritsch convective parameterization: An update. *J. Appl. Meteor.,* **43,** 170–181.

Liu, M., and J. J. Carroll, 1996: A high-resolution air pollution model suitable for dispersion studies in complex terrain. *Mon. Wea. Rev.,* **124,** 2396–2409.

Mass, C. F., and Coauthors, 2003: Regional environmental prediction over the Pacific Northwest. *Bull. Amer. Meteor. Soc.,* **84,** 1353–1366.

Mlawer, E. J., S. J. Taubman, P. D. Brown, M. J. Iacono, and S. A. Clough, 1997: RRTM, a validated correlated-k model for the longwave. *J. Geophys. Res.,* **102,** 16 663–16 682.

Noh, Y., W. G. Cheon, S. Y. Hong, and S. Raasch, 2003: Improvement of the K-profile model for the planetary boundary layer based on large eddy simulation data. *Bound.-Layer Meteor.,* **107,** 401–427.

Pino, D., J. Vilà-Guerau de Arellano, and P. G. Duynkerke, 2003: The contribution of shear to the evolution of a convective boundary layer. *J. Atmos. Sci.,* **60,** 1913–1926.

Pleim, J. E., 2007: A combined local and nonlocal closure model for the atmospheric boundary layer. Part I: Model description and testing. *J. Appl. Meteor. Climatol.,* **46,** 1383–1395.

——, and J. S. Chang, 1992: A non-local closure model for vertical mixing in the convective boundary layer. *Atmos. Environ.,* **26A,** 965–981.

——, and A. Xiu, 1995: Development and testing of a surface flux and planetary boundary layer model for application in mesoscale models. *J. Appl. Meteor.,* **34,** 16–32.

——, and ——, 2003: Development of a land surface model. Part II: Data assimilation. *J. Appl. Meteor.,* **42,** 1811–1822.

Reisner, J., R. M. Rasmussen, and R. T. Bruintjes, 1998: Explicit forecasting of supercooled liquid water in winter storms using the MM5 mesoscale model. *Quart. J. Roy. Meteor. Soc.,* **124B,** 1071–1107.

Shafran, P. C., N. L. Seaman, and G. A. Gayno, 2000: Evaluation of numerical predictions of boundary layer structure during the Lake Michigan Ozone Study. *J. Appl. Meteor.,* **39,** 412–426.

Steeneveld, G. J., B. J. H. van de Wiel, and A. A. M. Holtslag, 2006: Modeling the evolution of the atmospheric boundary layer coupled to the land surface for three contrasting nights in CASES-99. *J. Atmos. Sci.,* **63,** 920–935.

Stull, R. B., 1984: Transilient turbulence theory. Part I: The concept of eddy mixing across finite distances. *J. Atmos. Sci.,* **41,** 3351–3367.

Troen, I., and L. Mahrt, 1986: A simple model of the atmospheric boundary layer: Sensitivity to surface evaporation. *Bound.-Layer Meteor.,* **37,** 129–148.

Vila-Guerau de Arellano, J., O. S. Vellinga, A. A. M. Holtslag, F. C. Bosveld, and H. Klein Baltink, 2001: Observational evaluation of PBL parameterizations modeled by MM5. Preprints, *11th PSU/NCAR MM5 Users' Workshop,* Boulder, CO, NCAR, 102–106.

Wilks, D. S., 1995: *Statistical Methods in the Atmospheric Sciences*. Academic, 467 pp.

Wisse, J. S. P., and J. V. G. de Arellano, 2004: Analysis of the role of the planetary boundary layer schemes during a severe convective storm. *Ann. Geophys.,* **22,** 1861–1874.

Xiu, A., and J. E. Pleim, 2001: Development of a land surface model. Part I: Application in a mesoscale meteorological model. *J. Appl. Meteor.,* **40,** 192–209.

Zhang, D. L., and W. Z. Zheng, 2004: Diurnal cycles of surface winds and temperatures as simulated by five boundary layer parameterizations. *J. Appl. Meteor.,* **43,** 157–169.

Zhong, S., H.-J. In, X. Bian, J. Charney, W. Heilman, and B. Potter, 2005: Evaluation of real-time high-resolution MM5 predictions over the Great Lakes region. *Wea. Forecasting,* **20,** 63–81.